Catalysis Letters, Vol. 114, Nos. 3–4, April 2007 (© 2007)
DOI: 10.1007/s10562-007-9062-4

Lithium ion-exchanged zeolite faujasite as support of iron catalyst for Fischer-Tropsch synthesis

Ping Wang, Jincan Kang, Qinghong Zhang, and Ye Wang*

State Key Laboratory of Physical Chemistry of Solid Surfaces, College of Chemistry and Chemical Engineering, Xiamen University, Xiamen 361005, P.R. China

Received 22 November 2006; accepted 16 January 2007

Among various microporous and mesoporous materials investigated, the Li^+-exchanged zeolite faujasite has been found to be the most efficient support of iron catalyst for producing C_5^+ hydrocarbon fuels via Fischer-Tropsch synthesis. The location of iron species in the catalyst is a key issue in obtaining high selectivities to C_5^+ hydrocarbons. It is proposed that the Li^+ cation and the supercage structure of zeolite faujasite both play important roles in improving the selectivities to C_5^+ hydrocarbons over the Fe catalyst.

KEY WORDS: Fischer-Tropsch synthesis; iron catalyst; lithium; zeolite faujasite; C_5^+ hydrocarbons.

1. Introduction

Fischer-Tropsch (FT) synthesis is a key reaction for the transformation of synthesis gas, which can be derived from natural gas, coal, or biomass, into hydrocarbon fuels. Researches on catalyst development for the production of hydrocarbon fuels based on FT synthesis have attracted renewed attention because of the urgent demand for the decrease in the dependency on oil [1,2]. Moreover, the hydrocarbon fuels produced in FT synthesis can be sulfur-free and ultra-clean, and may easily meet the stringent environmental requirements [2,3]. However, because FT synthesis usually follows the Anderson-Schultz-Flory product distribution, the design of catalysts with desired product selectivities remains a critical challenge [4–7].

Many recent studies have indicated interestingly that the utilization of microporous or mesoporous materials, which possess ordered porous structures, as catalyst supports can modify the product selectivities for the cobalt-catalyzed FT synthesis [8–15]. Moreover, interesting size effects of cobalt particles on activity and C_5^+ selectivity have recently been reported using carbon nanofiber-supported catalysts [16]. These studies have provided insights into the design of new Fischer-Tropsch catalysts with improved activity and tunable product distributions.

On the other hand, similar studies are very few for the iron-catalyzed FT synthesis. Because of the lower cost and some distinct features such as wider operation ranges of temperature and H_2/CO ratio, Fe-based catalysts could provide an attractive complement to Co-based catalysts for the purpose of producing ultra-clean hydrocarbon fuels via FT synthesis [17–20]. However, as compared with Co catalysts, Fe-based catalysts usually exhibit higher selectivities to CO_2 because of the higher activity toward the water gas shift reaction. This may lead to 30–50% of the carbon feed being rejected as CO_2 in some cases [4], and this is particularly unfavorable when the H_2-rich synthesis gas is used. Moreover, Fe catalysts generally give lower selectivities to C_5^+ hydrocarbons as compared with Co and Ru catalysts especially in the absence of heavy modifications using modifiers such as copper and potassium.

Recently, we have systematically investigated the catalytic behaviors of Fe catalysts supported on various microporous and mesoporous materials. Our aim is to gain insights into possible effects of supports with ordered porous structures on the product distributions over Fe catalysts. We found that the use of zeolite faujasite could provide higher selectivities to C_5^+ hydrocarbons than the use of other porous materials as the supports of Fe. To the best of our knowledge, this is the first report on the significant enhancing effect of zeolite faujasite support on C_5^+ selectivity over a Fe-based catalyst although there exist scarce studies on the use of faujasite as the support of Fe for CO hydrogenation [21]. The present paper reports the unique role of zeolite faujasite support in determining the product distributions of supported Fe catalysts in FT synthesis. The influences of cations in the ion-exchange position, catalyst preparation and pretreatment methods on catalytic behaviors are also discussed.

*To whom correspondence should be addressed.
E-mail: wangye@xmu.edu.cn

2. Experimental

The faujasite (NaX with a Si/Al ratio of 1.3 and NaY with a Si/Al ratio of 2.8) and other type zeolites in Na-form were purchased from Nankai Catalyst Co. or prepared by hydrothermal synthesis in our laboratory [11]. The H-form or other alkali metal ion-exchanged zeolites (mainly zeolite Y) were prepared by ion exchange of the Na-form samples with aqueous solution of NH_4NO_3 (1 M) or alkali metal acetate, followed by drying and calcination at 823 K. The contents of Li and K in the Li^+- and K^+-exchanged zeolite Y samples (LiY and KY), which were measured by ICP technique, were 1.99 and 10.1 wt%, respectively. These corresponded to ion-exchange degrees of 68 and 62% for the LiY and KY, respectively. By measuring the content of the remaining Na in the zeolite HY, we evaluated the ion-exchange degree for this sample, and we obtained a value of 66%. The crystalline structure of each zeolite before and after ion exchange was confirmed by X-ray diffraction measurements. Mesoporous materials including MCM-41, MCM-48, and SBA-15 were prepared by hydrothermal synthesis using the procedures described in literature [22,23]. A non-porous fumed silica (Cab–O–Sil, denoted as SiO_2 hereafter) purchased from Acros Organics was used for comparison.

The loading of iron onto each support was typically carried out with an incipient wetness impregnation method using an ethanol solution of $Fe(NO_3)_3$ unless otherwise stated, and the loading amount of iron was generally 10 wt%. The volume of the solution was kept close to the pore volume of the support. The sample was calcined at 773 K after the solvent (ethanol) was removed by drying in vacuum at 313 K.

FT synthesis was carried out with a fixed-bed flow reactor operated at 2.0 MPa. To make good comparisons with the Co catalysts supported on microporous and mesoporous materials, in this work, we adopted reaction conditions close to those used for the Co catalysts except for a higher reaction temperature (543 K). The catalyst (typically 0.8 g) loaded in the reactor was first reduced in H_2 flow at 723 K for 30 h. The synthesis gas with a H_2/CO ratio of 2 was then introduced into the reactor after the temperature was decreased to 543 K. Argon with a concentration of 4% contained in the synthesis gas was used as an internal standard for the calculation of CO conversion. The products were analyzed by two on-line gas chromatographs (GCs) equipped with a capillary column (PONA) and two packed columns (Porapak Q and Molecular Sieve 5A). All the lines and valves between the exit of the reactor and the GCs were heated to 543 K. The qualitative identification of the C_6–C_{30} hydrocarbon products was also performed by GC-MS analysis. The results at steady state, typically after 10 or 15 h of reaction, were shown here and used for discussion.

X-ray diffraction (XRD) measurements were carried out with a Phillips X'pert Pro Super X-ray diffractometer with Cu-K_α radiation and X'Celerator detection systems. The transmission electron microscopy (TEM) was carried out in a FEI Technai 30 electron microscope (Phillips Analytical) operated at an acceleration voltage of 300 kV.

3. Results and discussion

3.1. FT synthesis over Fe catalysts supported on various microporous and mesoporous materials

Table 1 shows the catalytic behaviors of Fe catalysts supported on various ordered microporous and mesoporous materials as well as SiO_2 with a Fe loading amount of 10 wt% for FT synthesis. It should be noted that we have *not* calculated hydrocarbon selectivities on a CO_2-free basis although such calculation was used in most studies for Fe-based catalysts. As compared with the Co catalysts loaded on similar supports [15], most of these Fe-based catalysts showed lower selectivities to C_5^+ hydrocarbons (especially C_{10}–C_{20} hydrocarbons) but higher ones to C_2–C_4 and CO_2. It was unexpected that the Fe catalysts supported on MCM-41 and MCM-48 were almost inactive for CO hydrogenation, and the Fe/SBA-15 showed a similar activity and selectivity pattern to the Fe/SiO_2, whereas the Co catalysts supported on mesoporous materials exhibited superior activities and selectivities for the formation of C_5^+ hydrocarbons [10, 13–15].

On the other hand, although the Fe catalysts supported on several microporous zeolites such Na-ZSM-5, Na-MOR (Na-mordenite), and Na-BEA (Na-beta zeolite) do not possess the advantage in C_5^+ formation over the Fe/SiO_2, it is of interest to find that, the use of zeolite faujasite (NaX or NaY zeolite) as the support of Fe catalyst can significantly increase the C_5^+ selectivity. As shown in figure 1, the comparison of detailed product distributions among several supported Fe catalysts revealed that the formations of C_{10}–C_{28} hydrocarbons over the Fe/NaX and Fe/NaY were enhanced at the expense of C_1–C_4 hydrocarbons. We have evaluated the carbon-chain growth probability (α) using the equation of Anderson-Schulz-Flory distribution, i.e., $M_n = (1-\alpha)\alpha^{n-1}$, where M_n and n represent the molar fraction of each hydrocarbon product and the carbon number, respectively [7]. The α values calculated from the slope of the curves of ln M_n versus n for the Fe/NaX and Fe/NaY catalysts were remarkably higher than other supported Fe catalysts (table 1).

It is known that Na-ZSM-5 possesses a two-dimensional channel structure with cages at the crossing of the zigzag and the straight channels, which are 0.55 nm × 0.51 nm and 0.53 nm × 0.56 nm in dimensions, respectively. The porous structure of zeolite

Table 1
Effect of supports on catalytic behaviors of Fe catalysts in FT synthesis[a]

Catalyst[b]	CO conv. (%)	Selectivity (%)[c]							αα
		CO_2	CH_4	C_2–C_4	C_5–C_9	C_{10}–C_{20}	C_{21}^+	C_5^+	
Fe/SiO_2	22	12	15	40	29	4.1	0.1	33	0.66
Fe/MCM-41	<1.0	–	–	–	–	–	–	–	–
Fe/MCM-48	2.0	26	25	38	11	0	0	11	0.50
Fe/SBA-15	17	11	14	40	29	6.2	0.3	35	0.62
Fe/Na-ZSM-5	3.0	19	14	48	19	0	0	19	0.51
Fe/Na-MOR	29	20	12	35	23	7.0	3.2	33	0.63
Fe/Na-BEA	5.8	24	16	46	14	0	0	14	0.48
Fe/NaX	48	30	5.6	18	24	18	5.1	47	0.77
Fe/NaY	49	21	7.8	23	23	17	8.9	48	0.76

[a] Reaction conditions: $H_2/CO = 2$, $T = 543$ K, $P = 2$ MPa.
[b] Fe content was 10 wt %.
[c] Carbon balance was better than 95%.

mordenite can be viewed as a one-dimensional channel system with pore diameter of 0.65 nm × 0.70 nm containing side pockets where a part of the ion-exchange cations are sitting. The channel system of both zeolites may restrict the diffusion of large and long-chain paraffin molecules. Zeolite beta possesses a three-dimensional channel structure with relatively larger pore diameters, but the Si/Al ratio of this zeolite is much higher than that of the faujasite. The distinct feature of zeolite faujasite is its supercage structure. There exist large voids called supercages of ca. 1.3 nm in diameter in the faujasite, and the size of windows of these supercages is ca. 0.7 nm. We speculate that the peculiar structure might enhance the re-adsorption of reaction intermediates, and thus might result in the increase in the chain growth probability.

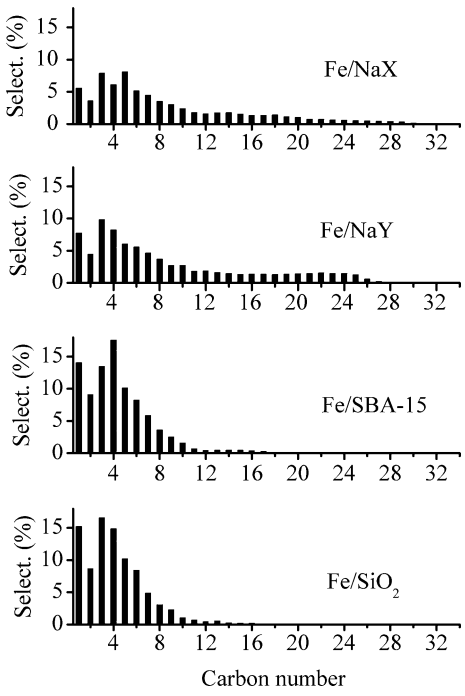

Figure 1. Product distributions over Fe/NaX, Fe/NaY, Fe/SBA-15 and Fe/SiO_2 catalysts.

3.2. Influences of cations on catalytic behaviors

Subsequently, we investigated the influences of cations located in the ion-exchange position in zeolite faujasite on catalytic behaviors. Table 2 summarizes the catalytic performances of Fe catalysts supported on zeolite Y with different cations. For comparison, the catalytic results over the alkali metal ion-modified Fe/SiO_2 catalysts (alkali metal/Fe = 0.04) have also been listed in the table. It is well known that the modification of Fe catalysts with an alkali metal ion (especially K^+) could suppress CH_4 formation and modify the selectivities to higher hydrocarbons [24]. As shown in table 2, the modification of the Fe/SiO_2 with alkali metal ions really increased the selectivities to C_5^+ hydrocarbons and decreased those to C_2–C_4 hydrocarbons and/or CH_4. The C_5^+ selectivity reached 43% over the K^+-Fe/SiO_2 catalyst.

As compared with the Fe/SiO_2, the Fe/HY also exhibited a higher C_5^+ selectivity, confirming that the supercage of zeolite Y played roles in enhancing the formation of higher hydrocarbons. The use of an alkali metal ion-exchanged zeolite Y as the support provided a higher CO conversion and a lower CH_4 selectivity than the Fe/HY. The CO conversion increased remarkably with changing the alkali metal ion from Li^+ to Cs^+. However, the increase in the selectivity to CO_2 was also remarkable at the same time, and the CO_2 selectivity reached 41% over the Fe/CsY catalyst. In other words, the water gas shift reaction took place seriously over this catalyst, and a large proportion of CO was consumed to give CO_2. This also caused a considerable drop in C_5^+ selectivity over the Fe/KY and Fe/CsY catalysts. As a result, the highest C_5^+ selectivity was achieved over the Fe/LiY catalyst. It is of interest that the selectivities to CO_2 and CH_4 are both the lowest over this catalyst.

Table 2
FT synthesis over Fe catalysts supported on zeolite Y and SiO_2 with different cations[a]

Catalyst[b]	CO conv. (%)	Selectivity (%)[c]							$\alpha\alpha$
		CO_2	CH_4	C_2–C_4	C_5–C_9	C_{10}–C_{20}	C_{21}^+	C_5^+	
Fe/HY	27	12	15	24	28	11	2.9	42	0.68
Fe/LiY	40	8.6	6.7	16	27	26	16	69	0.84
Fe/NaY	49	21	7.8	23	23	17	8.9	48	0.76
Fe/KY	75	36	8.3	23	19	9.7	3.9	33	0.74
Fe/CsY	91	41	9.3	20	19	7.8	3.3	30	0.65
Fe/SiO_2	22	12	15	40	29	4.1	0.1	33	0.66
Li^+-Fe/SiO_2	21	12	18	30	25	12	2.5	40	0.73
Na^+-Fe/SiO_2	24	19	13	28	27	12	1.5	40	0.74
K^+-Fe/SiO_2	27	22	9.1	26	24	15	3.7	43	0.75

[a] Reaction conditions: $H_2/CO = 2$, $T = 543$ K, $P = 2$ MPa.
[b] Fe content was 10 wt %.
[c] Carbon balance was better than 95%.

However, as seen in table 2, the Li^+-Fe/SiO_2 catalyst did not exhibit peculiar catalytic performances as compared with the Na^+-Fe/SiO_2 and K^+-Fe/SiO_2 catalysts. The CO conversion and C_5^+ selectivity over the Li^+-Fe/SiO_2 were much lower than those over the Fe/LiY. Figure 2 further showed that the formation of longer-chain hydrocarbons with carbon numbers of C_{10}–C_{30} was significantly enhanced over the Fe/LiY catalyst. Therefore, the presence of Li^+ and the peculiar structure of the zeolite faujasite may both play crucial roles in obtaining higher selectivities to C_5^+ hydrocarbons over the Fe/LiY catalyst.

3.3. *Influences of preparation and pretreatment methods on catalytic behaviors of Fe/LiY catalysts*

Because cations such as Na^+ and Li^+ in zeolite faujasite can only occupy several positions located in the supercages, sodalite cases and hexagonal prisms [25], the location of Fe in the zeolite may be a key issue if the interaction between Fe species and Li^+ is crucial. Moreover, the functioning of the supercage structure should also depend on the location of iron in the catalyst. To uncover the influence of Fe location, we have investigated the catalytic properties of three Fe/LiY catalysts prepared by different methods using the same starting materials, i.e., $Fe(NO_3)_3$ and LiY. The Fe/LiY catalyst described above was prepared by the incipient wetness impregnation method using an ethanol solution of $Fe(NO_3)_3$, followed by drying and calcination (see the experimental section, denoted as Fe/LiY-*iw* hereafter). The other two Fe/LiY catalysts were prepared by the conventional wet impregnation of LiY in an excess amount of aqueous solution of $Fe(NO_3)_3$ (denoted as Fe/LiY-*wi*) and by the mechanical mixing of $Fe(NO_3)_3$ and LiY in agate mortar (denoted as Fe/LiY-*mm*). The Fe/LiY-*wi* and Fe/LiY-*mm* were dried and calcined under the same conditions with those used for the Fe/LiY-*iw*. Table 3 shows that the Fe/LiY-*iw* catalyst exhibits a significantly higher C_5^+ selectivity as well as lower CO_2 and CH_4 selectivities than the Fe/LiY-*wi* and the Fe/LiY-*mm* catalysts. From the detailed product distributions shown in figure 3, we could see that the Fe/LiY-*iw* catalyst provided significantly higher selectivities to hydrocarbons with longer carbon chains, especially C_{10}–C_{30} than the other two catalysts.

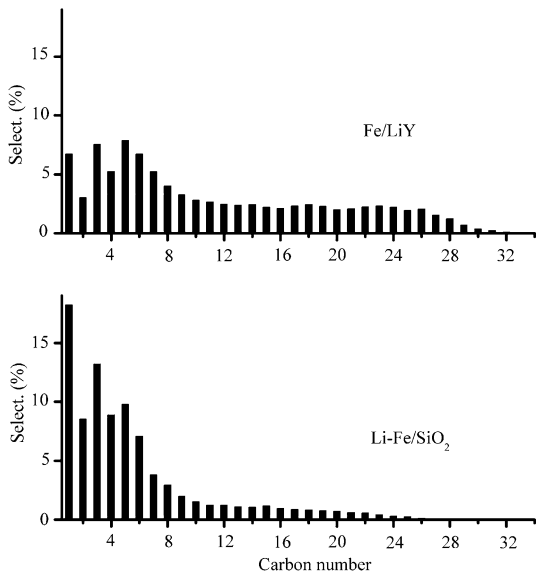

Figure 2. Product distributions over Fe/LiY and Li-Fe/SiO_2 catalysts.

We have characterized these three Fe/LiY catalysts. XRD patterns for the three catalysts (figure 4) did not show significant differences. Only diffraction peaks ascribed to the crystalline structure of the zeolite Y were observed for all these samples. The absence of any Fe-related phases suggested that the iron species might be well dispersed in the zeolite or might exist in amorphous states after calcination or maybe our XRD measurements using Cu-K_α radiation were not very sensitive to the iron oxide phase. However, we can see distinct differences in the TEM images for these samples. As shown in figure 5, we observed many large iron oxide

Table 3
FT synthesis over Fe/LiY catalysts prepared by different methods[a]

Catalyst[b]	CO conv. (%)	Selectivity (%)[c]							αα
		CO_2	CH_4	C_2–C_4	C_5–C_9	C_{10}–C_{20}	C_{21}^+	C_5^+	
Fe/LiY-*iw*	40	8.6	7.6	16	27	26	16	69	0.84
Fe/LiY-*wi*	35	18	15	30	23	12	2.7	37	0.72
Fe/LiY-*mm*	47	28	15	28	22	7.3	1.0	30	0.65

[a] Reaction conditions: $H_2/CO = 2$, $T = 543$ K, $P = 2$ MPa.
[b] Fe content was 10 wt %.
[c] Carbon balance was better than 95%.

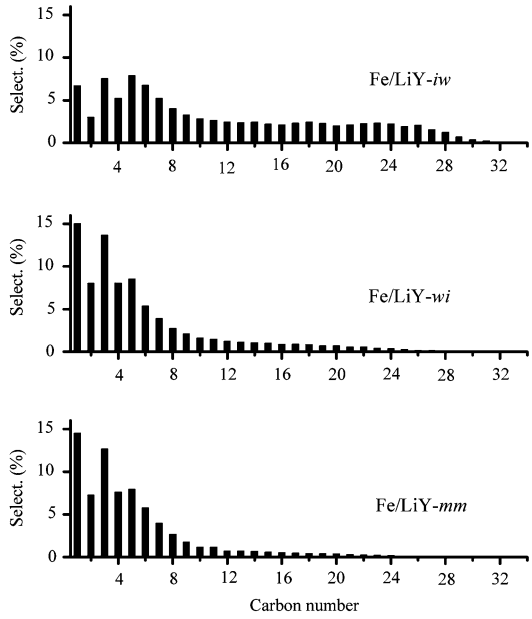

Figure 3. Product distributions over the Fe/LiY catalysts prepared by different methods.

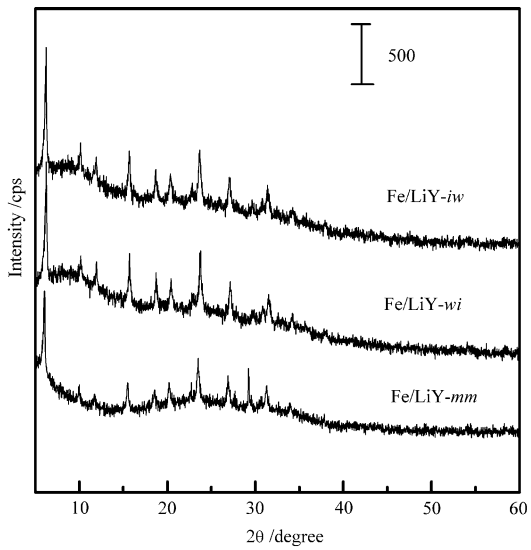

Figure 4. XRD patterns of the Fe/LiY catalysts prepared by different methods.

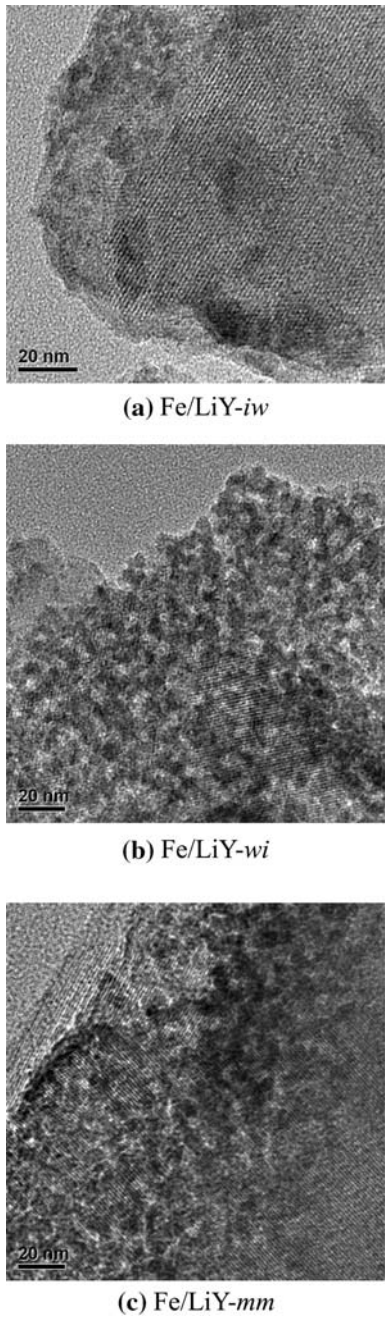

Figure 5. TEM images of the Fe/LiY catalysts prepared by different methods.

particles with sizes of ca. 5–20 nm over the Fe/LiY-*wi* and Fe/LiY-*mm* samples (figure 5b, c), suggesting that most of the iron species in these two samples might not enter the pores of the zeolite and might be located outside the supercages after calcination. On the other hand, such large iron oxide particles were fewer over the Fe/LiY-*iw* sample (figure 5a). We speculate that a larger part of iron species might be incorporated into the supercages of zeolite in this sample. Therefore, it is probable that the finely dispersed Fe species in zeolite LiY are very unique for obtaining the high C_5^+ selectivity in FT synthesis.

It should be mentioned that it took about 10 h to reach a steady state for the Fe/LiY-*iw* catalyst (figure 6). Both the CO conversion and the C_5^+ selectivity did not undergo significant changes after a further 15 h of reaction. It is well known that iron catalysts are usually

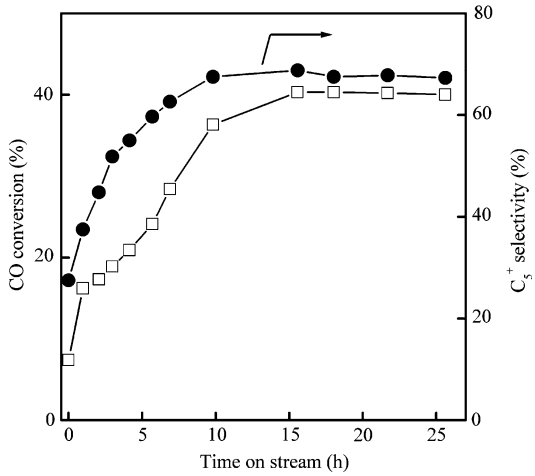

Figure 6. Changes in catalytic performances with time on stream over the Fe/LiY-*iw* catalyst.

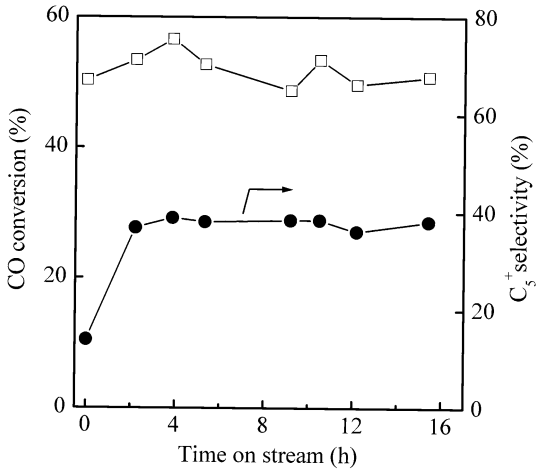

Figure 7. Changes in catalytic performances with time on stream over the Fe/LiY-*iw* catalyst after CO pretreatment at 573 K for 15 h.

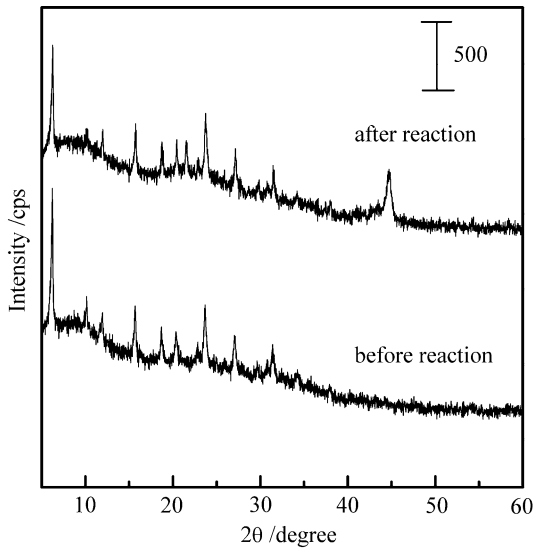

Figure 8. XRD patterns of the Fe/LiY-*iw* catalyst before and after the reaction.

reconstructed to form iron carbides under the reaction conditions in FT synthesis [20,26]. Thus the long induction period in figure 6 may correspond to such a catalyst reconstruction process. It has also been reported that, for a precipitated iron catalyst modified with copper and potassium, the pretreatment of catalyst with CO could increase the initial CO conversion and favored the formation of higher hydrocarbons [27]. We have investigated the influence of pretreatment of our Fe/LiY-*iw* catalyst with CO at 573 K for 15 h after the H_2 reduction. It can be seen from figure 7 that, although the catalytic performance can reach steady state after only ca. 2 h of reaction, the C_5^+ selectivity was much lower than that observed in figure 6. Therefore, it seems that the Fe/LiY-*iw* catalyst requires to be reconstructed under reaction conditions (synthesis gas flow) to obtain the optimum catalytic performances.

To gain insight into the structure change of the Fe/LiY-*iw* catalyst during the reaction, we have carried out XRD measurement for the Fe/LiY-*iw* catalyst after a 25 h of reaction under the conditions of Table 3. As shown in figure 8, a new diffraction peak at 2θ of 44.7° can be clearly observed after the reaction. This peak is assignable to an iron carbide (Fe_7C_3) phase. Thus, it can be speculated that the iron carbide species is formed in the initial reaction stage and may be responsible for the FT synthesis as suggested in literature [20, 26].

4. Conclusions

We found that the zeolite faujasite-supported Fe catalysts exhibited remarkably higher selectivities to C_5^+ hydrocarbons (especially C_{10}–C_{30} hydrocarbons) in FT synthesis than the Fe catalysts supported on other microporous and mesoporous materials investigated.

The cations in the ion-exchange position of zeolite faujasite also exerted significant effects on the catalytic performances, and the Li^+-exchanged zeolite faujasite was the best support of iron catalyst for the production of C_5^+ hydrocarbons. Simultaneously, the Fe/LiY catalyst showed the lowest selectivities to CO_2 and CH_4. The catalytic performances of the Fe/LiY catalyst were strongly dependent on the preparation method, which probably resulted in Fe species in different locations in the catalyst. Both the interactions between the Fe species and the Li^+ cations and the supercage structure of zeolite faujasite were proposed to play pivotal roles in improving the catalytic performances.

Acknowledgments

This work was supported by the National Natural Science Foundation of China (Nos. 20373055), the National Basic Program of China (No. 2005CB221408), the Scientific Research Foundation for the Returned Oversea Chinese Scholars (grant to Q.Z.), and the Program for New Century Excellent Talents at the University of China (NCET-040602, grant to Y.W.).

References

[1] J.R. Rostrup-Nielsen, Catal. Rev. 46 (2004) 247.
[2] H. Schulz, Appl. Catal. A 186 (1999) 3.
[3] M. Yamada and Y. Ohtsuka, Catal. Today 89 (2004) 387.
[4] S. Soled, E. Iglesia and R.A. Fiato, Catal. Lett. 7 (1990) 271.
[5] C.H. Bartholomew, Catal. Lett. 7 (1990) 303.
[6] E. Iglesia, Appl. Catal. A 161 (1997) 59.
[7] G.P. van der Laan and A.A.C.M. Beenackers, Catal. Rev. 41 (1999) 255.
[8] A.Y. Khodakov, A. Griboval-Constant, R. Bechara and V.L. Zholobenko, J. Catal. 206 (2002) 230.
[9] K. Okabe, M. Wei and H. Arakawa, Energy Fuels 17 (2003) 822.
[10] Y. Ohtsuka, Y. Takahashi, M. Noguchi, T. Arai, S. Takasaki, N. Tsubouchi and Y. Wang, Catal. Today 89 (2004) 419.
[11] Q. Tang, Q. Zhang, P. Wang, Y. Wang and H. Wan, Chem. Mater. 16 (2004) 1967.
[12] Y. Wang, H. Wu, Q. Zhang and Q. Tang, Microporous Mesoporous Mater. 86 (2005) 38.
[13] H. Li, S. Wang, F. Ling and J. Li, J. Mol. Catal. A 244 (2006) 33.
[14] H. Li, J. Li, H. Ni and D. Song, Catal. Lett. 110 (2006) 71.
[15] Q. Tang, P. Wang, Q. Zhang and Y. Wang, Chem. Lett. 35 (2006) 366.
[16] G.L. Bezemer, J.H. Bitter, H.P.C.E. Kuipers, H. Oosterbeek, J.E. Holewijn, X. Xu, F. Kapteijn, A.J. van Dillen and K.P. de Jong, J. Am. Chem. Soc. 128 (2006) 3956.
[17] M.E. Dry, Catal. Lett. 7 (1990) 241.
[18] L. Xu, S. Bao, R.J. O'Brien, A. Raje and B.H. Davis, Chemtech (1998) 47.
[19] S. Li, S. Krishnamoorthy, A. Li, G.D. Meitzner and E. Iglesia, J. Catal. 206 (2002) 202.
[20] H. Schulz, T. Riedel and G. Schaub, Catal. Lett. 32 (2005) 117.
[21] L. Guczi and I. Kiricsi, Appl. Catal. A 186 (1999) 375.
[22] J.S. Beck, J.C. Vartuli, W.J. Roth, M.E. Leonowicz, C.T. Kresge, K.D. Schmitt, C.T.-W. Chu, D.H. Oslen, E.W. Sheppard, S.B. McCullen, J.B. Higgins and J.L. Schlenker, J. Am. Chem. Soc. 114 (1992) 10834.
[23] D. Zhao, J. Feng, Q. Huo, N. Melosh, G.H. Fredrickson, B.F. Chmelka and G.D. Stucky, Science 279 (1998) 548.
[24] A.P. Raje, R.J. O'Brien and B.H. Davis, J. Catal. 180 (1998) 36.
[25] S. Buttefey, A. Boutin, C. Mellot-Draznieks and A.H. Fuchs, J. Phys. Chem. B 105 (2001) 9569.
[26] J.B. Butt, Catal. Lett. 7 (1990) 61.
[27] D.B. Bukur, L. Nowicki, R.K. Manne and X. Lang, J. Catal. 155 (1995) 366.